Nonsequential and Sequential Dual Detection Probe Lateral Flow Immunoassay Device for Staphylococcal Enterotoxin B Detection

Paquito E. Relox[1*], Katherine Ann C. Israel[2], Yuki Hiruta[3] and Daniel Citterio[3]

[1]Institute of Aquatic and Applied Sciences
Davao del Norte State College
Panabo City, Davao del Norte 8105 Philippines
[*]*paquito.relox@dnsc.edu.ph*

[2]College of Agriculture and Food Science
University of the Philippines Los Baños
College, Laguna 4031 Philippines

[3]Department of Applied Chemistry
Keio University
Yokohama, Kanagawa 223 – 8522 Japan

Date received: August 5, 2024
Revision accepted: December 12, 2024

Abstract

Staphylococcal enterotoxins (SEs) are among the leading causes of foodborne illnesses in the Philippines. Rapid and sensitive detection of these toxins in food, particularly staphylococcal enterotoxin B (SEB) – the most potent type of SE – is imperative. Rapid toxin detection can be achieved using a lateral flow immunoassay (LFIA) device. However, low sensitivity has been a persistent issue with LFIA devices. To develop an LFIA device with improved sensitivity, this study investigated the exclusive use of antibodies as biorecognition molecules in a dual-detection probe LFIA device format and the configuration of the LFIA device to release the probes nonsequentially and sequentially. The LFIA device was fitted with two layers of glass fiber sample pads, loaded separately with the two detection probes, and partially separated by a Scotch tape film. For the nonsequential LFIA device, the two sample pads were pretreated with blocking buffers containing the same sugar concentration, whereas for the sequential LFIA device, the two sample pads were pretreated with blocking buffers containing different sugar concentrations. When tested against a filtered, homogenized durian candy sample, the nonsequential LFIA device generated higher signal intensity than the sequential LFIA device. This result suggests that aggregation of the detection probes was superior to sequential binding in enhancing the signal of the LFIA device for SEB detection. The sensitivity of the nonsequential LFIA device at 5 ng/mL was two-fold higher compared to previous POCT LFIA devices for SEB detection in food samples.

Keywords: lateral flow immunoassay, sequential detection probe delivery, dual detection probe, nonsequential, indirect ELISA

1. Introduction

Staphylococcal enterotoxins (SEs), produced by *Staphylococcus aureus*, have been identified by Azanza *et al.* (2019) as the second leading cause of foodborne disease in the Philippines. Notably, in 2015, approximately 2,000 individuals in the Caraga Region suffered from staphylococcal food poisoning after consuming durian candy (Geronimo, 2015). The production of the toxin occurs when the *S. aureus* population exceeds 10,000 colony-forming units (cfu) per gram of food (BC Centre for Disease Control, 2024). This level is above the acceptable limit of 100 cfu/g for bacteria in products such as durian candy (Food and Drug Administration, 2013). Hence, the presence of SEs indicates poor handling practices that render food unsafe for consumption. Among the SEs, the B type (SEB) is the most potent, with an oral effective dose (ED50) of 0.3 µg/kg (Office of Biological Safety – University of Wisconsin Madison, n.d.). Due to its heat resistance, SEB can persist in thermally processed foods (Fries and Varshney, 2013). Early and rapid detection of this toxin in the food chain, as part of quality control and product monitoring, can help prevent or reduce the occurrence of staphylococcal food poisoning incidents.

This can be implemented using point-of-care testing (POCT) devices, such as lateral flow immunoassay (LFIA) devices. A device qualifies as POCT when it satisfies the affordable, sensitive, specific, user friendly, rapid and robust, equipment free, and deliverable to end-users (ASSURED) criteria set by the World Health Organization (WHO). The highest sensitivity attained by LFIA devices developed for SEB detection in food samples, without an additional signal amplification step after sample application, was 10 ng/mL (Boyle *et al.*, 2010; Tsui *et al.*, 2013; Chiao *et al.*, 2013; Wu *et al.*, 2020).

Lateral flow immunoassay devices can be categorized into single-detection and dual-detection modes. Single-detection mode approaches include visual detection, luminescence detection, surface-enhanced Raman scattering (SERS) detection, and electrochemical detection. A typical LFIA device that relies purely on visual detection uses a label, such as gold nanoparticles, to produce the positive signal at the test line. An example of such an LFIA device is the pregnancy test kit (Khelifa *et al.*, 2022). Unlike the direct visual detection approach, luminescence detection generates a visual signal through the reaction between a substrate and an enzyme (Wang *et al.*, 2020). One reaction exploited for this purpose is between luciferin and luciferase, which is the light-generation mechanism found in fireflies (Bergua *et al.*, 2021).

Luminescence is best observed in the dark. Meanwhile, integrating SERS into LFIA generally involves the use of gold nanoparticles as detection probes further functionalized with Raman reporters. A Raman spectrometer measures the SERS signal from the probes (Wang *et al.*, 2017). With electrochemical detection, the LFIA device incorporates an electrochemical transducer, such as screen-printed electrodes. This miniaturized transducer converts biochemical events into electrical signals, which are then measured by an electrochemical reader. Depending on the LFIA setup, the presence of the target analyte can cause a decrease (signal-off) or an increase (signal-on) in signal intensity (Cheng *et al.*, 2022).

On the other hand, approaches that implement dual detection modes include colorimetric and SERS, colorimetric and enzymatic, and colorimetric and magnetic methods (Mahmoudi *et al.*, 2019). The combination of colorimetric and SERS enables the visual detection of the target analyte, which can then be confirmed and quantified by SERS. To achieve this, nanoparticles with visual and resonance properties, such as gold nanoparticles, are utilized as labels (Atta *et al.*, 2024). An example of the application of colorimetric and enzymatic detection methods is the use of gold nanoparticles functionalized with enzymes. The gold nanoparticles provide a direct visual signal, which can be enhanced by the colored product of the enzymatic reaction (e.g., horseradish peroxidase and 3,3',5,5'-tetramethylbenzidine [TMB]), as demonstrated in the study of Parolo *et al.* (2013). Lateral flow assay devices can also use magnetic nanoparticles as labels instead of gold nanoparticles. In addition to the visual signal provided by the black-colored magnetic nanoparticles, their magnetic field can be detected and quantified using a magnetic reader, with the strength of the magnetic field proportional to the concentration of the analyte of interest (Moyano *et al.*, 2020). Improvements in the sensitivity of LFIA devices, while retaining simplicity and cost-effectiveness, are likely to focus on visual signal amplification. Other modes may require the integration of instruments, which demand technical expertise for their use.

Among the recent approaches to visual signal enhancement of LFIA devices are the use of different nanogold morphologies, gold enlargement, silver deposition, and the use of magnetic nanoparticles as labels (Yang *et al.*, 2017; Razo *et al.*, 2018; Lu *et al.*, 2019). Still under visual signal enhancement is the utilization of dual gold conjugates in lateral flow immunoassay devices, as first reported by Choi *et al.* (2010). In this format, the second conjugate has an affinity for the first conjugate, which displays an affinity for the target

antigen. As the sample is applied and moves through the sample pad and conjugation pads, a second-conjugate–first-conjugate–antigen complex is formed. This complex is then captured at the test line to create a positive signal (Shen *et al.*, 2013). A dual gold conjugate LFIA device for thrombin achieved a sensitivity of 0.25 nM compared to the 7.5 nM sensitivity of a conventional LFIA device. Another study reported a 2.5-fold increase in prostate-specific antigen (PSA) sensitivity due to dual gold conjugate enhancement (Rodríguez *et al.*, 2016). None of the previous dual-detection-probe LFIA device studies exclusively used antibodies as biorecognition molecules that can mimic the interaction in indirect enzyme-linked immunosorbent assay (ELISA).

The dual gold probe/conjugate format amplifies the signal through complex formation or aggregation, wherein a larger number of gold nanoparticles accumulate on the test line. However, excessive aggregation can elevate the risk of a false positive response, as encountered when a primary conjugate of biotin-antibody-magnetic nanoparticles aggregated upon reacting with AuNP-streptavidin (Razo *et al.*, 2018). Rodríguez *et al.* (2016) avoided this scenario by applying the secondary detection probe separately to allow sequential binding. However, regarding user-friendliness, this would not be a good option. A dual detection probe LFIA device that can sequentially release the detection probes, even with a one-step sample application, could address these concerns. Several studies have integrated the sequential flow of reagents in lateral flow immunoassay devices. So far, only two works have offered simple and single linear LFIA devices capable of sequential reagent delivery. Panraksa *et al.* (2021) developed an LFIA to detect C-reactive protein, which demonstrated a modest but effective method to release three reagents sequentially. Three different channels were drawn on the nitrocellulose membrane by wax printing. The delay channel, located at the center between two non-delay tracks, was embedded with wax-printed baffles that stretched the total distance and time the liquid had to travel to reach the detection zone. This established the sequential flow of reagents with only a single application step. Also, wax printing developed an LFIA device for a model mouse IgG assay with a sequential flow of reagents imitating ELISA. The wax barrier, printed into half the depth of the filter paper sample pad, caused a delay in the rehydration and release of the pre-deposited enzyme substrate while allowing the unimpeded flow of the alkaline phosphatase-labeled anti-mouse IgG antibody (Ishii *et al.*, 2018).

To create a sensitive LFIA device for detecting SEB in durian candy samples, this study explored the fabrication of novel and facile designs for dual

detection probe LFIA devices with nonsequential and sequential release configurations. The study aimed to achieve this while maintaining the linear and miniature structure of the LFIA devices. Additionally, the dual detection probe/conjugate in the LFIA devices utilized antibodies exclusively, a novel approach not previously undertaken. The performance of the nonsequential and sequential LFIA devices was compared, and the sensitivity of the design with superior performance was assessed.

2. Methodology

2.1 Chemicals and Instruments

The monoclonal anti-staphylococcal enterotoxin B antibody from mouse (ASM; SAB4200859), anti-mouse IgG antibody from rabbit (AMR; SA5-10192), and polyclonal anti-staphylococcal enterotoxin B antibody from rabbit (ASR; S9008), as well as 40 nm gold nanoparticles in 0.1 mM PBS (753637) and cellulose fiber pad (CFSP 203000), were all obtained from Merck Millipore, United States. Lyophilized, highly pure staphylococcal enterotoxin B (BT 202), was purchased from Toxin Technology, Inc., Florida, United States. The nitrocellulose membrane (Whatman™ FF80HP) and glass fiber pad (Ahlstrom 8964) were procured from Cytiva, United States and Ahlstrom-Munksjö, United States, respectively. The plastic cassette used was sourced from DCN Diagnostics, Inc., United States.

The Silhouette Cameo 3 was used to cut A4-sized nitrocellulose membranes into 25 mm strips. The compact cutter from Fujishoko Machinery Co., LTD was employed to produce 4 mm-wide strips of the sample-conjugation pad, nitrocellulose membrane, and absorbent pad. Photo images of the LFIA devices were captured using a scanner (9000F Mark II, Canon, Japan).

2.2 Preparation of Lateral Flow Immunoassay Device Components

2.2.1 Gold Nanoparticles (AuNP) - Antibody Conjugates

The AuNP and antibody were conjugated according to the procedure described by Anfossi *et al.* (2011) with some modifications. To produce the AuNP-ASM conjugates (primary detection probe), 1 mL of AuNP (OD 1) was mixed with 40 μL of 0.1 mg/mL ASM. The conjugation was performed for 1 h under ambient conditions while shaken at 200 rpm using an IKA MS 3 digital orbital shaker. To block the remaining bare surfaces of the AuNP, 115

µL of 10% BSA and 15 µL of 0.01% Tween-20 were added. Blocking required an additional 1 h of incubation. To recover the AuNP-ASM pellets, the solution was centrifuged at 7000 x g for 10 min. The pellets were washed twice with 1X PBS (pH 7.4) containing 0.20% Tween-20. The washed conjugate pellet was resuspended in 20 mM BB, pH 8.5, containing 1% BSA, 0.25% Tween-20, 2% sucrose, and 0.02% NaN3, and adjusted to an OD 4 concentration. To prepare the AuNP-AMR (secondary detection probe), the same steps were followed, except that the amount of antibody conjugated to 1 mL of AuNP was 10 µL of 0.1 mg/mL antibody and 20 µL of 0.1 mg/mL antibody.

2.2.2 Preparation of the Nitrocellulose Membrane and Absorbent Pad

The Whatman FF80HP fast-flow membrane was used to fabricate the LFIA device with sequential release of detection probes. A 25 mm FF80HP strip was adhered to a backing card and cut into 4-mm strips. About 1 µL of capture antibody solution (0.5 mg/mL in 10 mM PB with 0.03% SDS) and 1 µL of control spot antibody solution (0.5 mg/mL in 10 mM PB with 0.03% SDS) were spotted at 31.25 and 23.75 mm from the absorbent pad end of the NC membrane, respectively. The strips were dried at 37 °C for 2 h and then stored in a desiccator with < 20% RH. The absorbent pad (CFSP 203000), cut into 4 x 20 mm, was used without pretreatment.

2.3 Fabrication and Testing of Nonsequential and Sequential Lateral Flow ImmunoAssay Device (LFIA) Formats

The lateral flow immunoassay device with a sequential flow feature was assembled as depicted in Figure 1. Two glass fiber pads (4 x 20 mm) constituted the sample pad. The glass fiber sample pads also functioned as conjugate pads. The first layer (bottom) sample-conjugate pad was pre-treated with 20 µL of conjugate pad-blocking buffer (20 mM BB containing 1% BSA, 0.25% Tween-20, 2% sucrose, and 0.02% NaN3). The blocking buffer was applied at the front end of the sample pad. On the other hand, 20 µL of conjugate pad-blocking buffer with 2, 4, 6, and 8% sucrose concentrations were applied 5 mm from the front end of the second layer (upper) sample-conjugate pads. After blocking, the sample-conjugate pads were dried at 37 °C for 2 h and then stored in a desiccator with < 20% RH.

The first layer of the sample-conjugate pad had a 5 mm overlap with the nitrocellulose membrane. Scotch tape was placed 8 mm from the rear end of the strip, over the first layer of the sample-conjugate pad. The second layer of

the sample-conjugate pad was then laid over the first layer of the sample-conjugate pad and the scotch tape.

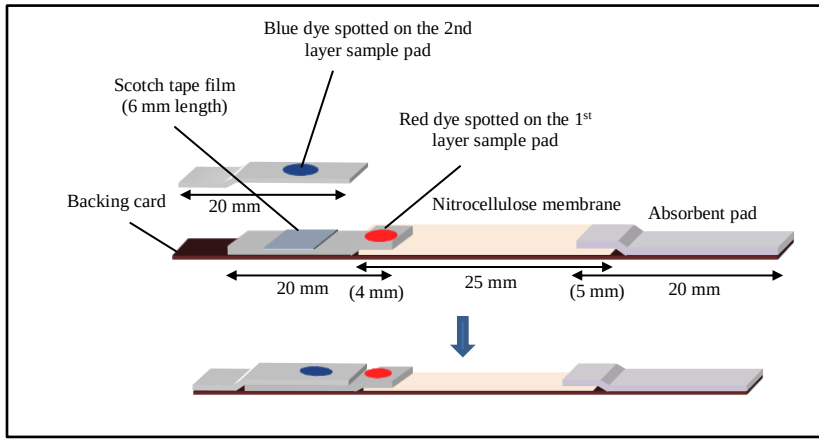

Figure 1. Schematic diagram of lateral flow assay device capable of sequential flow of two detection probes

The layers of the sample pad had a 16 mm overlap, with only the first layer of the sample pad in contact with the NC membrane. The absorbent pad crossed over the NC membrane with a 5 mm overlap. The assembled strips were then housed in a plastic cassette.

The LFIA device with a nonsequential release configuration was constructed in the same manner as the sequential format. However, in this case, the upper layer of the sample-conjugate pad was pretreated with conjugate pad blocking buffer (CPBB), a specific chemical, to enhance the performance of the device. This treatment involved a 2% sucrose concentration.

To visualize the sequential flow of liquid through the two layers of sample-conjugate pads, the first layer of the sample-conjugate pad was spotted with 1 µL of 10% red dye (McCormick Red Food Coloring), while the second layer was spotted with 1 µL of 10% blue dye (McCormick Blue Food Coloring). The pads were then dried at 37 °C for 1 h.

To confirm the sequential flow and examine the effect of increasing sucrose concentrations in the second layer sample pad/conjugate pad blocking buffer, the LFIA strips were applied with 150 µL of running buffer. The time it took for the dyes to reach the test spot region was recorded. The test was performed in triplicates.

2.4 Sample Preparation

To prepare the 1:5 (durian candy: sample buffer) blank sample, 1 g of durian candy was homogenized with 5 mL of sample buffer. The homogenized sample was filtered using cotton treated with 1X PBS containing 1% BSA. Meanwhile, to prepare the 1:5 spiked sample, a 1:4 homogenized sample was prepared first. Then, the sample was spiked with SEB to a final concentration of 150 ng/mL at a 1:5 sample dilution. The homogenized and SEB-spiked sample was incubated at ambient temperature for at least 1 h before segregating the residues by cotton filtration.

2.5 Individual Optimization of the Primary Detection and Secondary Detection Probes in the Dual Detection Probe LFIA Device Format

The first and second layers of glass fiber sample pads were pretreated and blocked with CPBB as described previously. The first- and second-layer sample pads were blocked with 20 µL of CPBB containing 2 and 8% sucrose, respectively. In the optimization of the primary probe (ASM-AuNP), different quantities were tested: 12.5, 15, 17.5, and 20 µL. The concentration of the detection probe was OD 4. The primary detection probe was deposited in the blocked area of the first layer of the sample pad.

On the other hand, the optimization of the secondary detection probe involved the use of AMR-AuNP, produced by conjugating 1 mL of OD 1 AuNP (40 nm) with 10 and 20 µL of 0.1 mg/mL antibody. The secondary detection probe was deposited in the blocked area of the second layer of the sample pad. After depositing the conjugates, the sample pads were dried for 2 h at 37 °C and cured overnight. Similar to the optimization of the primary probe, the dual detection probe LFIA device format was used to optimize the secondary detection probe, with only the secondary detection probe present in the sample pad. Tabulated below are the different treatments for the optimization of the secondary detection probe.

The dual detection probe LFIA devices were assembled following the previously described procedure. Assays using the blank and spiked 1:5 homogenized and filtered durian candy samples were performed on triplicate LFIA devices per treatment. A total of 150 µL of the samples were applied to the LFIA devices for 20 min. The LFIA devices were visually inspected, and the signal intensity of the scanned images was measured using the ImageJ software developed by Rasband (2022) of the National Institute of Health ([NIH], United States).

Table 1. Secondary detection probe optimization treatments

AMR load	Volume (μL)			
	2.5	3.5	4.5	5.5
1 μg AMR/mL AuNP OD1	T1	T2	T3	T4
2 μg AMR/mL AuNP OD1	T5	T6	T7	T8

2.6 Determination of the Optimal Combination of the Primary and Secondary Detection Probes in Sequential Dual Detection Probe LFIA Device Format

The individually optimized quantities of the primary and secondary detection probes using the durian candy samples were incorporated into the sequential dual detection probe LFIA device format. The dual detection probe LFIA devices were prepared using the individually optimized quantities of the primary and secondary detection probes, as well as the cumulative quantity of the two detection probes, with the optimized quantity of the secondary detection probe already accounted for. The objective of the latter was to determine whether the dual detection probe configuration would generate a stronger positive signal compared to using a single detection format with the same quantity of detection probes.

Per treatment, assays were performed on triplicate LFIA devices for both blank and spiked 1:5 homogenized and filtered durian candy samples. The assay used 150 μL of sample with a 20-min run time. The LFIA devices run with blank samples were immediately checked for a false positive signal, while the LFIA devices run with spiked samples were scanned, and the capture antibody spot signal intensities were measured using ImageJ software.

2.7 Performance Comparison between the Nonsequential and Sequential Dual Detection Probe Lateral Flow Immunoassay Devices

Nonsequential and sequential dual detection probe LFIA devices were assembled following the described procedure. The determined optimal combination of the primary and secondary detection probes in the sequential format was also used for the nonsequential format. The blank and spiked durian candy samples were run on triplicate LFIA devices for each dual detection probe LFIA device format. A total of 150 μL of samples were assayed onto the LFIA devices. The LFIA devices were visually inspected after a 20-min run time.

2.8 Evaluation of the Sensitivity of the Dual Detection Probe LFIA Device

The sensitivity of the dual detection probe LFIA device format (nonsequential) was evaluated against the sensitivity of an LFIA device format

with only the primary detection probe present, but with the same configuration as the dual detection probe LFIA device format. The nonsequential dual detection probe LFIA devices were prepared following the previously described method, which involved identifying the optimal combination of the primary and secondary detection probes.

In the case of the LFIA device format with only the primary detection probe, the amount of the primary detection probe applied to the first layer sample pad was equivalent to the sum of the amounts of the primary and secondary detection probes used in the dual detection probe format.

The sensitivities of the nonsequential dual detection probe LFIA device and its version with only the primary detection probe were evaluated using 1:5 homogenized and filtered durian candy samples with the following SEB concentrations: 0 (control), 1, 5, 10, 20, 50, and 100 ng/mL. Each sample was run on triplicate LFIA devices. The sample volume assayed was 150 µL, with a run time of 20 min.

2.9 Data Analysis

The LFIA devices were visually inspected after the 20-min run time. The devices were then scanned using the Canon 9000F Mark II scanner. The signal intensity of the LFIA test spot was measured against the background signal. Using ImageJ software (Maryland, United States), the scanned image of the LFIA strip was inverted, and the gray values of the test spot and background were recorded. The test spot signal intensity (S/N) was calculated as the ratio of the test spot's gray value (signal) to the background's gray value (noise). Signal intensities between treatments or devices were statistically compared using one-way analysis of variance (ANOVA) and the t-test. These statistical analyses were performed using SPSS Software (International Business Machines Corporation [IBM], 2025).

3. Results and Discussion

3.1 Sequential Delivery in a Dual Detection Probe LFIA Device

Two layers of sample pads, separated by a scotch tape film, were employed to allow sequential detection probe delivery in the lateral flow immunoassay device. The scotch tape splits the sample's flow into two paths: one through the first layer and the other through the second layer. The sample that enters

the second layer flows more slowly due to the higher sugar content of its CPBB. The portion of the sample passing through the second layer with the secondary detection probes eventually descends to the front end of the first layer. From there, it travels across the NC membrane by capillary action toward the absorbent pad (Figure 2). The speed of the sample flow depends on the sucrose concentration of the CPBB applied to the sample pads, as illustrated in Figure 3.

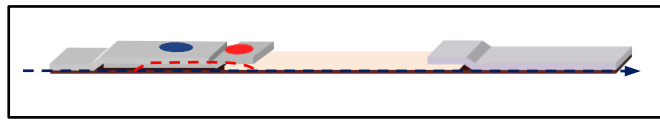

Figure 2. Scheme of the one-step sequential detection probe delivery of the fabricated LFIA device with two layers of sample pad

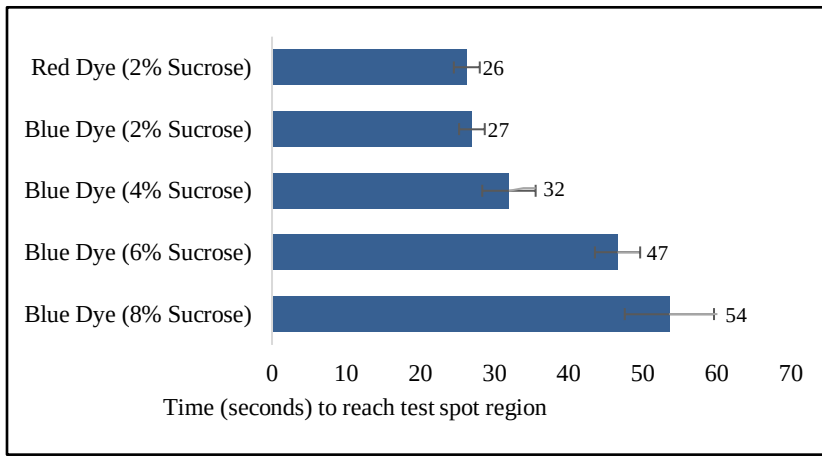

Figure 3. Time of the dye to reach the test spot region

The delay in the flow of the portion of the sample passing through the second layer sample pad was dictated by the percentage of sucrose in the CPBB used, as reflected in Figure 3. Application of 150 µL of running buffer (20 mM borate buffer, pH 8.5, with 1% BSA, 1.0% Tween-20, and 0.02% NaN3) showed that an increase in the percentage of sucrose in the CPBB of the second layer sample pad resulted in an increase in the time required for the blue dye to reach the test spot region. This can be attributed to the increase in viscosity brought about by the higher sugar concentration (Kim, 2016). At higher

viscosity, the sample flowed more slowly, requiring more time to reach the test spot region.

Figure 4 shows the sequential flow of the blue dye (second layer) and red dye (first layer) through the LFIA device. When the CPBB of the first- and second-layer sample-conjugate pads had similar sucrose content (2%), the sample flowed through the two layers of the sample pad at the same pace, as indicated by the almost equal time for the red dye and blue dye to reach the test spot region. In this case, no sequential flow occurred.

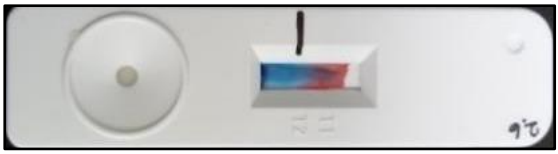

The marker line on the cassette points to the location of the test spot of the LFIA device.

Figure 4. Simulated sequential flow of detection probes through the LFIA device using food coloring dyes

A complete sequential flow of the reagents/dyes/detection probes in this format cannot be achieved because these reagents are generally not released simultaneously. The secondary detection probe could catch up with the primary detection probe before it reaches the test spot region. However, the mixing of the two detection probes can be minimized by widening the flow gap between the two layers of the sample pad, further increasing the difference in sucrose concentration between the CPBB of the second layer sample pad and the first layer sample pad. Before this study, only two LFIA devices capable of sequential reagent delivery, which did not dramatically deviate from the classical LFIA design, had been devised (Ishii *et al*., 2018; Panraksa *et al*., 2021). Ishii *et al*. (2018) developed an LFIA device with a printed thin wax barrier in the sample pad to delay the flow of the enzyme-substrate. On the other hand, in the work of Panraksa *et al*. (2021), they introduced wax-printed non-delay and delay channels in the nitrocellulose membrane to enable the sequential flow of reagents. Unlike these previous methods, the current method did not require additional specialized equipment, such as a wax printer.

3.2 Optimization of the Primary Detection and Secondary Detection Probes in the Dual Detection Probe LFIA Device Format

The objective of the optimization test was to find the optimal amount of detection probe that would give the maximum signal intensity (S/N) in a

spiked sample while minimizing the false positive result in a blank sample. In this case, the optimal amount refers to the minimum amount of detection probe needed to achieve the maximum signal intensity.

3.2.1 Individual Optimization of the Detection Probes

Firstly, the optimal amounts of the primary and secondary detection probes were determined separately using filtered 1:5 durian candy as a sample. For this purpose, four different quantities of the primary detection probe (12.5, 15, 17.5, and 20 µL) were tested. As shown in Figure 5, the 20-µL quantity of the primary detection probe produced the maximal signal intensity. However, its signal intensity was not significantly different from the other quantities of the primary detection probe, based on the One-Way ANOVA analysis at 95% Confidence Interval (CI), which gave a P-value of 0.268. A summary of the One-Way ANOVA analysis results is shown in the table below.

Table 2. One-way ANOVA analysis results for the difference in signal intensities (S/N) of the LFIA devices with different amounts of primary detection probes

Treatments primary detection probe quantity (µL)	S/N mean value	Calculated F-value	Calculated P-value at 95% confidence interval
12.5	1.53		
15.0	1.55	1.581	0.268
17.5	1.55		
20.0	1.73		

Among the quantities tested, only the 12.5 µL quantity did not show a false positive signal (Figure 6). According to Zhang *et al.* (2020), larger amounts of detection probes can lead to increased nonspecific interactions that could result in false-positive signal generation. Aside from nonspecific interactions, the physical trapping of detection probe particles within the nitrocellulose membrane's pores could also produce a false positive signal. Since a false positive response is considered a limiting factor, 12.5 µL was considered the optimal amount of the primary detection probe.

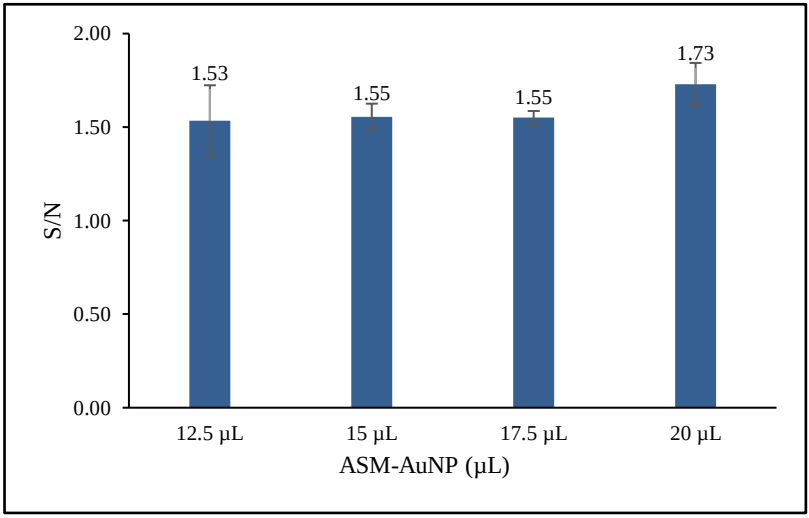

Figure 5. Signal intensity (S/N) measurements during the optimization of the primary detection probe

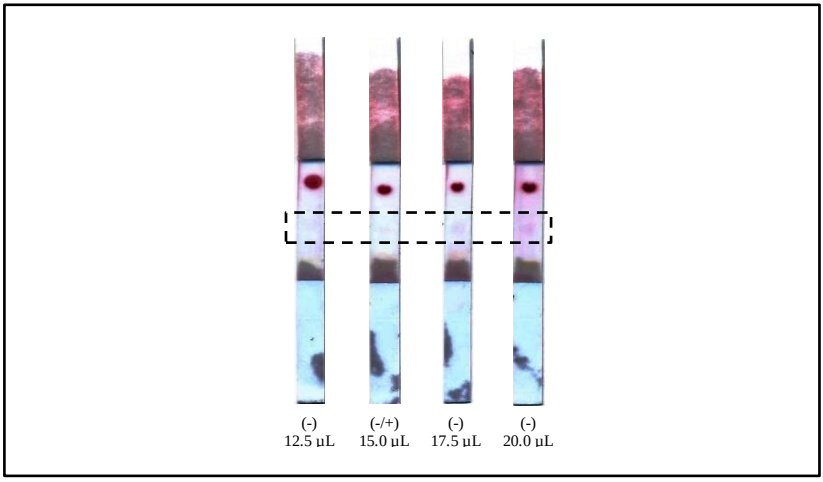

Figure 6. Representative LFIA devices with different quantities of the primary detection probe (ASM-AuNP) ran with blank filtered durian samples

On the other hand, the optimal amount of the secondary detection probe was determined by using two AuNP-AMR probes made from 1 mL of AuNP conjugated with 1 and 2 µg of AMR. It was hypothesized that conjugation of the secondary antibodies to AuNP below the saturation level would reduce the false positive signal intensity. The idea was that with a smaller population of detection probe antibodies, their frequency of interaction with the capture

antibody would decrease, resulting in a lower rate of nonspecific interactions. However, as shown in Table 3, identical results emerged from the two classes of second detection probes: 1 µg AMR/mL AuNP OD 1 and 2 µg AMR/mL AuNP OD 1. False positive signals appeared at 4.5 and 5.5 µL levels but remained non-detectable at 2.5 and 3.5 µL levels. This suggested that the level of antibody saturation of the AuNP did not substantially reduce nonspecific interactions and false-positive signal generation. It appeared that the quantity of detection probes is the most important factor influencing or controlling the false positive signal in the LFIA device. This confirmed that nonspecific interactions were more prevalent at larger amounts of the detection probe. Consequently, the use of smaller amounts of the secondary detection probes helped avoid the production of false positive signals.

Table 3. Secondary detection probe optimization results

AMR load	Volume (µL)			
	2.5	3.5	4.5	5.5
1 µg AMR/mL AuNP OD1	(-)	(-)	(+)	(+)
2 µg AMR/mL AuNP OD1	(-)	(-)	(+)	(+)

Given these results, the 3.5 µL was considered the optimized quantity of the 2nd detection probe for both classes of 2nd detection probes.

3.2.2 Combined Optimization of the Detection Probes

The dual detection probe LFIA devices were prepared from the combined individual optimized quantities of the primary and secondary detection probes, totaling 16 µL, and from the cumulative quantity of the two detection probes at 12.5 µL, where the 3.5 µL optimized quantity of the secondary detection probe had already been accounted for. The objective of the latter was to demonstrate whether the dual detection probe configuration would generate a stronger positive signal compared to using a single detection probe format at the same total quantity of detection probes. By visual examination, it was found that, aside from the control treatment, only the dual detection probe LFIA device format with 9 µL of the primary detection probe and 3.5 µL of the secondary detection probe (produced from 1 mL of AuNP conjugated with 1 µg of AMR) showed no false positive response. Again, this can be attributed to the propensity for nonspecific interactions that lead to false positive signals when higher quantities of detection probes are used. This treatment had the same total quantity of detection probes as the control. Still, as shown in Figure 7, it achieved higher positive signal intensity, though not significantly, based

on its P-value of 0.054 obtained from one-way ANOVA analysis at a 95% CI (Table 4). This suggests that the dual detection probe LFIA device format could enhance the positive signal intensity while minimizing the false positive result.

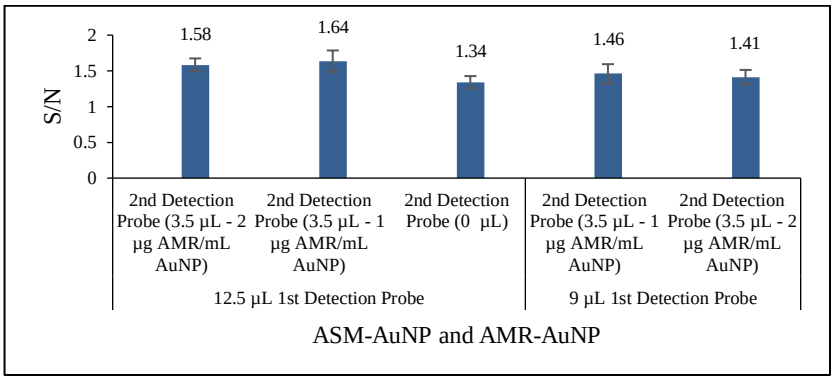

Figure 7. Dual detection probe LFIA optimization results

Table 4. One-way ANOVA analysis results for the difference in signal intensities (S/N) of the LFIA devices with different combinations of the primary and secondary detection probes

Treatments				
Quantity of 1st detection probe	Quantity of 2nd detection probe	S/N mean value	Calculated F-value	Calculated P-value at 95% confidence interval
12.5 µL	3.5 µL (2 µg AMR/mL AuNP)	1.58		
12.5 µL	3.5 µL (1 µg AMR/mL AuNP)	1.64		
12.5 µL	0 µL	1.34	3.311	0.057
9.0 µL	3.5 µL (1 µg AMR/mL AuNP)	1.46		
9.0 µL	3.5 µL (2 µg AMR/mL AuNP)	1.41		

Likewise, it was observed that the LFIA device with the secondary detection probe made from 1 µg AMR/mL of AuNP exhibited higher signal intensity than its counterpart with the secondary detection probe prepared from 2 µg

AMR/mL of AuNP. A possible explanation is that the lower AMR antibody saturation in the secondary detection probe increased the specific interaction ratio between the secondary detection probe and the primary detection probe. This could have occurred because more secondary detection probes can pack on a given space or volume to interact with the primary detection probes. Figure 8 illustrates what may have transpired in the scenario described above.

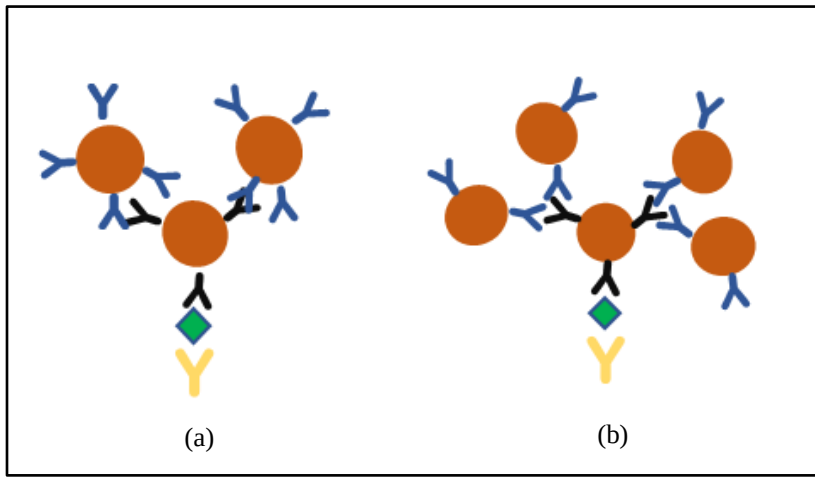

Figure 8. Interaction of less (a) and more AMR saturated (b) secondary detection probe with the primary detection probe

3.3 Performance of Nonsequential and Sequential Dual Detection Probe Lateral Flow Immunoassay Devices

The nonsequential LFIA device format was constructed similarly to the sequential format, except that the upper layer of the sample-conjugate pad was pretreated with CPBB containing a 2% sucrose concentration, instead of CPBB with 8% sucrose. In a sequential LFIA device, enhanced signal intensity occurs when the secondary detection probe binds to the primary detection probe that has already been immobilized in the capture antibody spot region. In contrast, the nonsequential LFIA device format allows the overlapping flow of primary and secondary detection probes, which results in aggregation of the probes before they reach the capture antibody spot region. This aggregation increases the signal intensity by creating larger detection probe complexes that emit stronger signals. Moreover, due to their larger size, aggregated detection probes tend to flow more slowly, prolonging their interaction with the antigen and capture antibody. As a result, more aggregated

detection probes bind to both the capture antibody and antigen, producing a stronger positive signal. However, the slower flow rate also increases the risk of a false positive signal. Similar observations were made in studies by Liu *et al.* (2011), who used MNP aggregates to reduce the detection limit of paraoxon methyl by 40-fold to 1.7 ng/mL, and Razo *et al.* (2018), who achieved a 32-fold sensitivity enhancement in detecting potato virus X by enlarging the MNP and AuNP complexes through aggregation. Additionally, Ren *et al.* (2019) reported a 1000-fold improvement in LFIA sensitivity for detecting *E. coli* O157:H7 by controlling AuNP aggregation.

Fortunately, during visual inspection, no false positive results were observed in the sequential and nonsequential dual detection probe LFIA devices when assayed with the blank sample. For both LFIA device formats, nonspecific interactions were minimized to prevent the generation of false positive signals. The average signal intensities for the two types of dual detection probe LFIA devices are shown in Figure 9. A t-test performed at a 95% confidence interval revealed that the nonsequential LFIA device format produced stronger positive S/N than the sequential LFIA device format, with a P-value of 0.011 (Table 5).

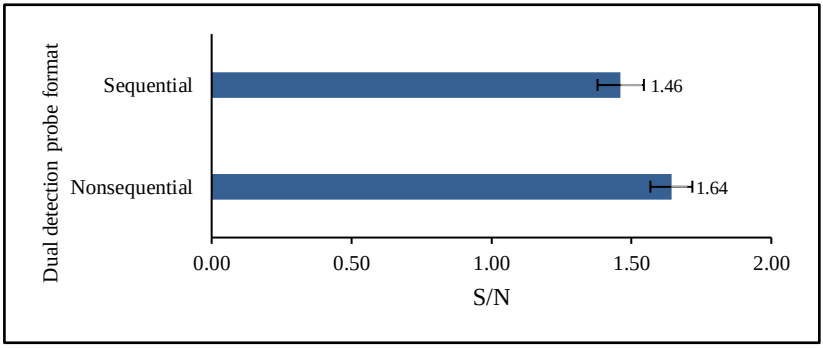

Figure 9. Comparison of the positive signal intensities (S/N) of the sequential and nonsequential dual detection probe LFIA device formats

Table 5. Independent t-test analysis results for the difference in S/N of the sequential and nonsequential dual detection probe LFIA devices

Type of dual detection probe LFIA device	S/N mean value	Calculated two-sided P-value at 95% confidence interval
Sequential	1.46	0.011
Nonsequential	1.64	

Based on this outcome, the nonsequential dual detection probe LFIA device format was found to be superior to the sequential dual detection probe LFIA device format. This suggests that, in this study, the aggregation of the first and second detection probes resulted in a stronger signal than their sequential binding. Consequently, the nonsequential dual detection probe LFIA device format was selected for the sensitivity assay. However, the one-step sequential LFIA device format could still be valuable for LFIAs that use detection probes with colorimetric enzymes as labels. These types of LFIAs require the sequential delivery of reagents for effective signal generation. The application of this format will not be limited to SEB detection but could extend to the detection of other important analytes.

3.4 Sensitivity of the Nonsequential Dual Detection Probe and Single Detection Probe LFIA Devices

The S/N measurements for the single detection probe and nonsequential dual detection probe LFIA devices, run with filtered 1:5 durian candy samples containing varying concentrations of SEB, are presented in Figure 10. The corresponding representative devices are shown in Figure 11.

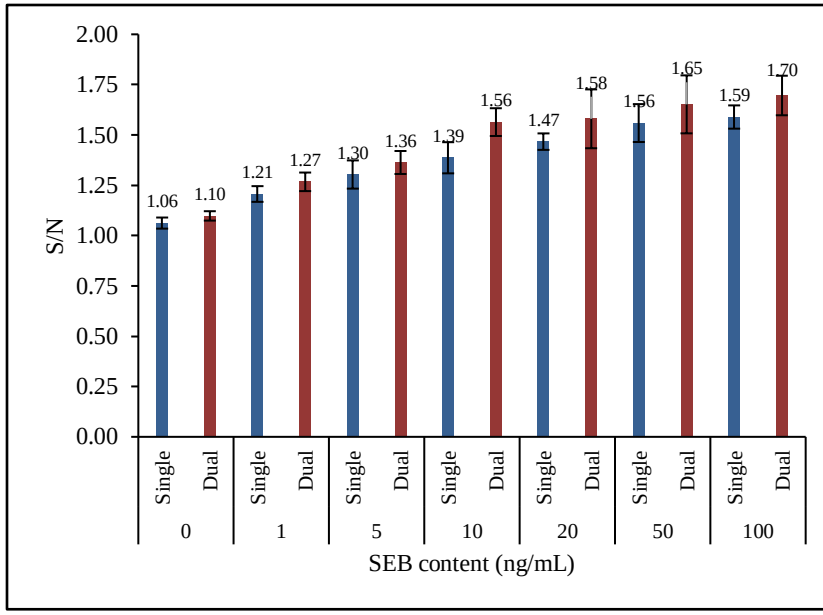

Figure 10. SEB concentration response of the single and dual detection probe LFIA device formats during a sensitivity test

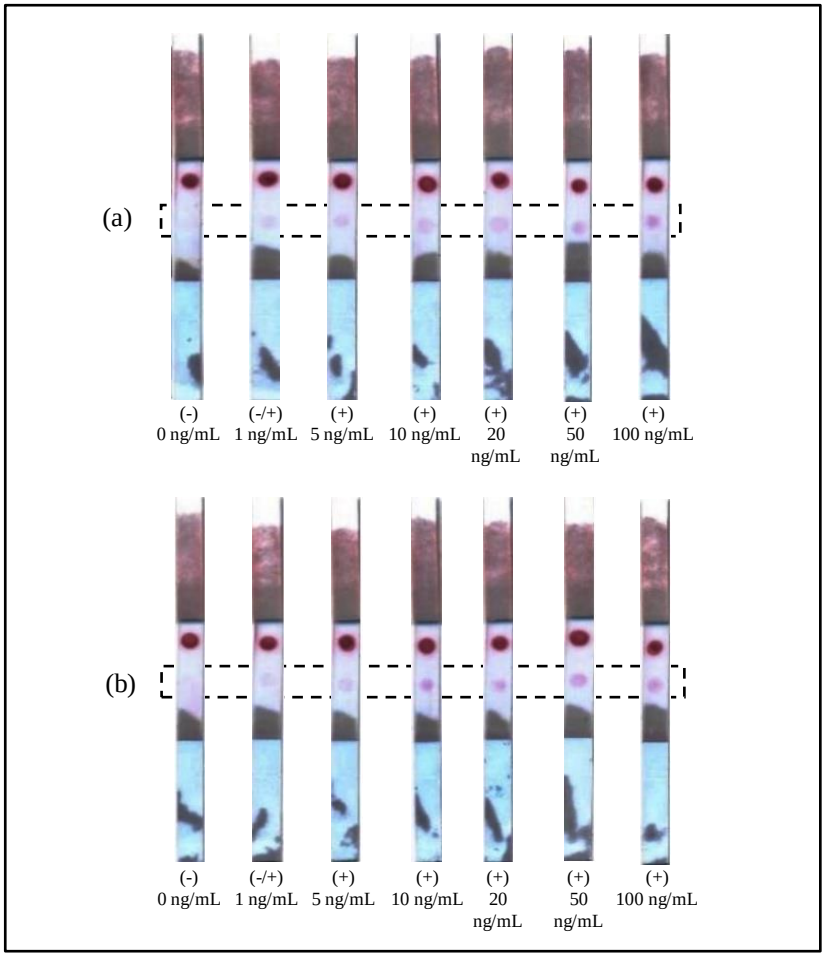

Figure 11. Representative LFIA devices of the single (a) and dual detection probes (b) LFIA devices run with samples with different concentrations of SEB during a sensitivity test

Although only statistically significant at a SEB concentration of 10 ng/mL when examined using the sample t-test at a 95% confidence level (Table 6), the dual detection probe LFIA device showed overall higher signal intensities across different SEB concentrations. Nevertheless, both the single and dual detection probe LFIA device formats had a visual limit of detection (vLOD) at 5 ng/mL.

Table 6. Independent t-test analysis results for the difference in signal intensities (S/N) of the single and dual detection probe LFIA devices

SEB concentration (ng/mL)	Type of LFIA device	S/N mean value	Calculated P-value at 95% confidence interval
0	Single	1.06	0.157
	Dual	1.10	
1	Single	1.21	0.170
	Dual	1.27	
5	Single	1.30	0.299
	Dual	1.36	
10	Single	1.39	0.038
	Dual	1.56	
20	Single	1.47	0.249
	Dual	1.58	
50	Single	1.56	0.394
	Dual	1.65	
100	Single	1.59	0.545
	Dual	1.70	

The S/N of the capture antibody spots for the single and nonsequential dual detection probe LFIA devices at 5 ng/mL ranged from 1.30 to 1.40. At this level of sensitivity, the LFIA devices in this study outperformed most LFIA devices from previous studies when tested against food samples. However, more sensitive detection of SEB is required to prevent the distribution of harmful food to consumers. Regarding the limitations of the LFIA devices in this study, they would not be effective or sensitive when analyzing colored samples such as tea candy, mangosteen candy, or chocolate-flavored milk products. Jung *et al.* (2020) also encountered this issue when they ran a spinach sample through their LFIA device to detect *E. coli* O157:H7. The green color of the spinach adversely affected the device's visual detection limit, as the pigments could mask or alter the color of the detection probes, impairing their visualization.

4. Conclusion and Recommendation

The results of this study demonstrated the feasibility of the dual detection probe LFIA device format, which relies solely on the interactions between antibodies, mimicking the signal amplification mechanism of indirect ELISA. As a result, a less complex and potentially cheaper dual detection probe lateral

flow immunoassay device can be produced, benefiting from the dual probe detection mechanism. A simpler LFIA device would facilitate easier and more economical reproduction, which is crucial for commercializing such a device. Moreover, the study successfully integrated a sequential delivery system with a dual detection probe in an LFIA device. This straightforward sequential delivery system, achieved by employing two layers of sample pads and controlling sample flow using blocking buffers with different sugar concentrations, can be easily replicated and applied to LFIA devices that use enzymatic reactions to generate signals. Adopting this mechanism in enzyme-based LFIA devices would allow for one-step sample application, in contrast to the two- or three-step application processes typically used. Additionally, the simplicity of the design would ensure the production of LFIA devices with consistent quality and performance. The dual detection probe LFIA in this study can operate with both sequential and non-sequential designs. In fact, the non-sequential design produced higher signal intensity than the sequential one. This suggests that aggregation is a more effective signal enhancement mechanism than the sequential binding of primary and secondary detection probes in the dual detection probe LFIA device used in this study. However, this result may vary with other combinations of antibodies. The non-sequential LFIA device had a visual limit of detection (vLOD) of 5 ng/mL for SEB in a 1:5 dilution of filtered durian candy, which is two-fold lower than most previous LFIA devices developed for SEB detection in food samples. This higher sensitivity will be beneficial for the early detection of SEB toxin in food samples, helping to prevent food poisoning. Nevertheless, the performance of the dual detection LFIA device could still be enhanced by evaluating other biorecognition molecules that offer higher signal intensity without causing nonspecific interactions.

5. Acknowledgement

This research project materialized with financial support from the Department of Science and Technology – Science Education Institute through its Accelerated Science and Technology Human Resource Development Program (ASTHRDP) and Research Enhancement Program (REP). This endeavor was partially supported by Davao del Norte State College through its study leave program for scholars.

6. References

Anfossi, L., D'arco, G., Calderara, M., Baggiani, C., & Giovannoli, C. (2011). Development of a quantitative lateral flow immunoassay for the detection of Aflatoxins in maize. Food Additives and Contaminants, 28(2), 226.

Atta, S., Zhao, Y., Li, J.Q., & Vo-Dinh, T. (2024). Dual-modal colorimetric and surface-enhanced Raman scattering (SERS)-based lateral flow immunoassay for ultrasensitive detection of SARS-CoV-2 using a plasmonic gold nanocrown. Analytical Chemistry, 96(12), 4783-4790.

Azanza, M.P.V., Membrebe, B.N., Sanchez, R.G., Estilo, E.E., Dollete, U.GM., Feliciano, R.G., & Garcia, N.K.A. (2019). Foodborne disease outbreaks in the Philippines (2005-2018). Philippine Journal of Science, 148(2), 317-336.

BC Centre for Disease Control. (2024). *Staphylococcus aureus* (food poisoning). Retrieved from http://www.bccdc.ca/health-info/diseases-conditions/staphylococcus-aureus

Bergua, J.F., Hu, L., Fuentes-Chust, C., Álvarez-Diduk, R., Hassan, A.H., Parolo, C., & Merkoçi, A. (2021). Lateral flow device for water fecal pollution assessment: from troubleshooting of its microfluidics using bioluminescence to colorimetric monitoring of generic *Escherichia coli*. Lab on a Chip, 21(12), 2417-2426.

Boyle, T., Njoroge, J.M., Jones, R.L., & Principato, M. (2010). Detection of staphylococcal enterotoxin B in milk and milk products using immunodiagnostic lateral flow devices. Journal of AOAC International, 93(2), 569-575. https://doi.org/10.1093/jaoac/93.2.569

Cheng, J., Yang, G., Guo, J., Liu, S., & Guo, J. (2022). Integrated electrochemical lateral flow immunoassays (eLFIAs): Recent advances. Analyst, 147(4), 554-570.

Chiao, D.J., Wey, J.J., Tsui, P.Y., Lin, F.G., & Shyu, R.H. (2013). Comparison of LFA with PCR and RPLA in detecting SEB from isolated clinical strains of *Staphylococcus aureus* and its application in food samples. Analytical Methods, 141, 1789-1795

Choi, D.H., Lee, S.K., Oh, Y.K., Bae, B.W., Lee, S.D., Kim, S., Shin, Y.B., & Kim, M.G. (2010). A dual gold nanoparticle conjugate-based lateral flow assay (LFA) method for the analysis of troponin I. Biosensors and Bioelectronics, 25(8), 1999-2002. https://doi.org/10.1016/j.bios.2010.01.019.

Office of Biological Safety – University of Wisconsin Madison (OBS-UWM). (n.d.). Staphylococcal Enterotoxin B (SEB). Retrieved from: https://ehs.wisc.edu/wp-content/uploads/sites/1408/2023/04/EHS-BIO-GUI-047-V02.pdf

Food and Drug Administration. (2013). FDA Circular No. 2013-010: Revised guidelines for the assessment of microbiological quality of processed foods, Philippines: Department of Health.

Fries, B.C., & Varshney, A.K. (2013). Bacterial toxins-Staphylococcal Enterotoxin B. Microbiology Spectrum, 1(2). https://doi.org/10.1128/microbiolspec.AID-0002-2012

Geronimo, J.Y. (2015, July 16). Poisoned durian candy contaminated with bacteria – DOH. Rappler. Retrieved from https://www.rappler.com/nation/99577-durian-candy-contaminatedbacteria

International Business Machines Corporation. (IBM). (2025). IBM SPSS free trial software. Retrieved from https://www.ibm.com/spss.

Ishii, M., Preechakasedkit, P., Yamada, K., Chailapakul, O., Suzuki, K., & Citterio, D. (2018). Wax-assisted one-step enzyme-linked immunosorbent assay on lateral flow test devices. Analytical Sciences, 34(1), 51-56. https://doi.org/10.2116/analsci.34.51

Jung, Y., Heo, Y., Lee, J.J., Deering, A., & Bae, E. (2020). Smartphone-based lateral flow imaging system for detection of food-borne bacteria *E. coli* O157:H7. Journal of Microbiological Methods, 168, 105800. https://doi.org/10.1016/j.mimet.2019.105800

Khelifa, L., Hu, Y., Jiang, N., & Yetisen, A. K. (2022). Lateral flow assays for hormone detection. Lab on a Chip, 22(13), 2451-2475.

Kim, E. (2010). Relationship between viscosity and sugar concentration in aqueous sugar solution using the Stokes' Law and Newton's First Law of Motion (Thesis). Faculty of Science, University of British Columbia, Vancouver, Canada.

Liu, C., Jia, Q., Yang, C., Qiao, R., Jing, L., Wang, L., Xu, C., & Gao, M. (2011). Lateral flow immunochromatographic assay for sensitive pesticide detection by using Fe_3O_4 nanoparticle aggregates as color reagents. Analytical Chemistry, 83(17), 6778-6784. https://doi.org/10.1021/ac201462d.

Lu, X., Mei, T., Guo, Q., Zhou, W., Lei, X., Chen, J., Zhou, X., Sun, N., & Fang, Z. (2019). Improved performance of lateral flow immunoassays for alpha-fetoprotein and vanillin by using silica shell-stabilized gold nanoparticles. Microchimica Acta, 186, 1-7.

Mahmoudi, T., de la Guardia, M., Shirdel, B., Mokhtarzadeh, A., & Baradaran, B. (2019). Recent advancements in structural improvements of lateral flow assays towards point-of-care testing. TrAC - Trends in Analytical Chemistry, 116, 13-30. https://doi.org/10.1016/j.trac.2019.04.016

Moyano, A., Serrano-Pertierra, E., Salvador, M., Martínez-García, J.C., Rivas, M., & Blanco-López, M.C. (2020). Magnetic lateral flow immunoassays. Diagnostics, 10(5), 288.

Panraksa, Y., Apilux, M., Jampasa, S., Puthong, S., Henry, C.S., Rengpipat, S., & Chailapakul, O. (2021). A facile one-step gold nanoparticles enhancement based on sequential patterned lateral flow immunoassay device for C-reactive protein detection. Sensors and Actuators B: Chemical, 329, 129241. https://doi.org/10.1016/j.snb.2020.129241

Parolo, C., de la Escosura-Muñiz, A., & Merkoçi, A. (2013). Enhanced lateral flow immunoassay using gold nanoparticles loaded with enzymes. Biosensors and Bioelectronics, 40(1), 412-416.

Rasband, W. (2022). ImageJ - Image processing and analysis in java [Computer software]. United States: National Institute of Health.

Razo, S.C., Panferov, V.G., Safenkova, I.V., Varitsev, Y.A., Zherdev, A.V., & Dzantiev, V.V. (2017). Double-enhanced lateral flow immunoassay for potato virus X based on a combination of magnetic and gold nanoparticles. Analytical Chimica Acta, 1007, 50-60. https://doi.org/10.1016/j.aca.2017.12.023

Ren, W., Mohammed, S.I., Wereley, S., & Irudayaraj, J. (2019). Magnetic focus lateral flow sensor for detection of cervical cancer biomarkers. Analytical Chemistry, 91(4), 2876-2884. https://doi.org/10.1021/acs.analchem.8b04848

Rodríguez, M.O., Covián, L.B., García, A.C., & Blanco-López, M.C. (2016). Silver and gold enhancement methods for lateral flow immunoassays. Talanta, 148, 272-278. https://doi.org/10.1016/j.talanta.2015.10.068.

Shen, G., Zhang, S., & Hu, X. (2013). Signal enhancement in a lateral flow immunoassay based on dual gold nanoparticle conjugates. Clinical Biochemistry, 46(16-17), 1734-1738. https://doi.org/10.1016/j.clinbiochem.2013.08.010

Tsui, P.Y., Chiao, D.J, Wey, J.J., Liu, C., Yu, C.P., & Shyu, R.H. (2013). Development of staphylococcal enterotoxin B detection strips and application of SEB detection strips in food. Journal of Medical Sciences (Taiwan), 33(5), 285-291. https://doi.org/10.6136/JMS.2013.33(5).285

Wang, X., Choi, N., Cheng, Z., Ko, J., Chen, L., & Choo, J. (2017). Simultaneous detection of dual nucleic acids using a SERS-based lateral flow assay biosensor. Analytical Chemistry, 89(2), 1163-1169.

Wang, D., He, S., Wang, X., Yan, Y., Liu, J., Wu, S., & Tang, Y. (2020). Rapid lateral flow immunoassay for the fluorescence detection of SARS-CoV-2 RNA. Nature Biomedical Engineering, 4(12), 1150-1158.

Wu, K.H., Huang, W.C., Shyu, R.H., & Chang, S.C. (2020). Silver nanoparticle-base lateral flow immunoassay for rapid detection of *Staphylococcal enterotoxin* B in milk and honey. Journal of Inorganic Biochemistry, 210(June), 111163.

Yang, Y., Ozsoz, M., & Liu, G. (2017). Gold nanocaged-based lateral flow immunoassay for immunoglobulin G. Mikrochim Acta, 184(7), 2023-2029.

Zhang, Y., Liu, X., Wang, L., Yang, H., Zhang, X., Zhu, C., & Li, B. (2020). Improvement in detection limit for lateral flow assay of biomacromolecules by test-zone pre-enrichment. Scientific Reports, 10(1), 9604. https://doi.org/10.1038/s41598-020-66456-1